Inorganic Chemistry

pubs.acs.org/IC
Article

Functionalization of Tetraphosphido Ligands by Heterocumulenes

Sebastian Hauer, Gábor Balázs, Fabian Gliese, Florian Meurer, Thomas M. Horsley Downie, Christoph Hennig, Jan J. Weigand, and Robert Wolf*

Cite This: https://doi.org/10.1021/acs.inorgchem.4c00808

ABSTRACT: Although numerous polyphosphido complexes have been accessed through the transition-metal-mediated activation and functionalization of white phosphorus (P_4), the selective functionalization of the resulting polyphosphorus ligands in these compounds remains underdeveloped. In this study, we explore the reactions between cyclotetraphosphido cobalt complexes and heterocumulenes, leading to functionalized P_4 ligands. Specifically, the reaction of carbon disulfide (CS_2) with [K(18c-6)][(Ar*BIAN)Co(η^4-P_4)] ([K(18c-6)]**1**, 18c-6 = [18]crown-6) affords the adduct [K(18c-6)][(Ar*BIAN)Co(η^3:η^1-P_4CS_2)] ([K(18c-6)]**3**), in which CS_2 is attached to a single phosphorus atom (Ar* = 2,6-dibenzhydryl-4-isopropylphenyl, BIAN = 1,2-bis(arylimino)acenaphthene diimine). In contrast, the insertion of bis(trimethylsilyl)sulfur diimide $S(NSiMe_3)_2$ into a P−P bond of [K(18c-6)]**1** yields [K(18c-6)][(Ar*BIAN)Co(η^3:η^1-$P_4SN_2(SiMe_3)_2$)] (K(18c-6)]**4**). This salt further reacts with Me_3SiCl to form [(Ar*BIAN)Co(η^3:η^1-$P_4SN_2(SiMe_3)_3$] (**5**), featuring a rare azatetraphosphole ligand. Moreover, treatment of the previously reported complex [(Ar*BIAN)Co(η^3:η^1-$P_4C(O)tBu$)] (**2**) with isothiocyanates results in P−C bond insertion, yielding [(Ar*BIAN)Co(η^3:η^1-$P_4C(S)N(R)C(O)tBu$)] (**6a,b**; R = Cy, Ph).

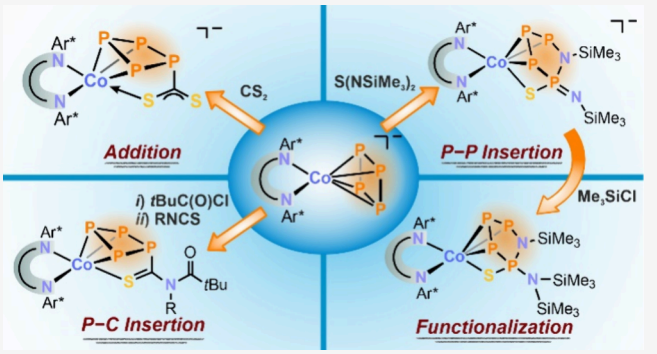

INTRODUCTION

The reaction of white phosphorus with transition metal complexes represents a powerful strategy in the synthesis of distinctive phosphorus-based compounds.[1] Transition-metal-mediated P_4 functionalization processes typically involve two principal steps, which have been subject to considerable investigation: Initially, a transition metal complex facilitates the cleavage of one or more P−P bonds of the P_4 tetrahedron, yielding metal complexes that incorporate an activated polyphosphido ligand. Subsequently, these P_n units undergo functionalization through reactions with suitable nucleophiles or electrophiles. The first step, P_4 activation, has been widely investigated and can result in a wide variety of polyphosphorus structures, with ligands containing from one to eight P atoms.[1] In particular, P_4 ligands such as [1.1.0]bicyclotetraphosphane-1,4-diide (commonly referred to as "butterfly-P_4^{2-}") and cyclotetraphosphide (*cyclo*-P_4^{2-}) units, emerge as prevalent structural motifs (see Figure 1a).[2,3] The subsequent functionalization of the coordinated P_n units typically constitutes a separate step.[1] While the reactivity in this step can vary based on the electronic properties of the transition metal fragment, it is generally acknowledged that functionalization of P_4 has not been as thoroughly explored as its activation.

Several routes for the functionalization of butterfly-P_4 complexes have been reported, including reactions such as the addition and insertion of nucleophiles and electrophiles (including alkylation), fragmentation, and transition metal coordination.[2,4] During our prior work, in which we reported the synthesis of the nickel butterfly-P_4 complex **A**, it was found that phenyl isothiocyanate (PhNCS) inserts into a P−P bond of the butterfly moiety. This reaction facilitated the formation of unusual bicyclo[3.1.0]heterohexane isomers **B** and **C** (Figure 1b).[2d,5]

While several *cyclo*-P_4 complexes have been reported, their reactivity has not been as extensively investigated as the butterfly-P_4 counterparts.[1,3] A study by Scheer and co-workers demonstrated that treatment of the *cyclo*-P_4 complex [Cp‴Co(η^4-P_4)] (**D**, Cp‴ = $C_5H_2tBu_3$) with carbon-centered nucleophiles leads to isomeric compounds **E** and **F** (Figure 1b).[6]

In a recent study, we reported the anionic *cyclo*-P_4 complex [(Ar*BIAN)Co(η^4-P_4)]$^-$ (**1**$^-$, Figure 1b) and its reaction with acyl chlorides, yielding the functionalized *cyclo*-P_4 complex [(Ar*BIAN)Co(η^3:η^1-$P_4C(O)tBu$] (**2**).[7] When compound **2** was treated with nitriles or isocyanides, there was a partial displacement of the $P_4C(O)R$ ligand from the cobalt center. Moreover, reaction with 2 equiv of KCN induced a [3 + 1]

Special Issue: Dialogue on Zintl Chemistry

Received: February 27, 2024
Revised: April 30, 2024
Accepted: May 9, 2024

https://doi.org/10.1021/acs.inorgchem.4c00808
Inorg. Chem. XXXX, XXX, XXX−XXX

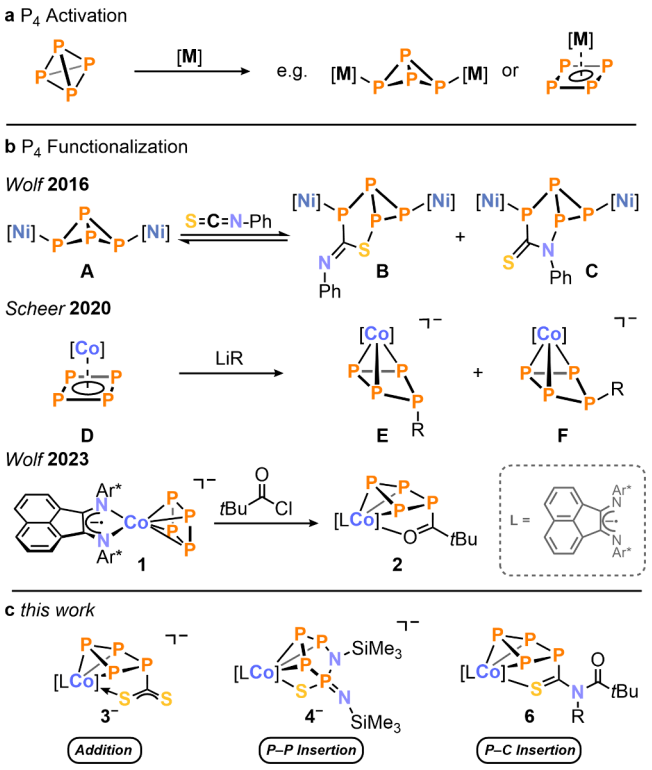

Figure 1. (a) Activation and (b) functionalization of white phosphorus; [Ni] = [CpNi(IMes)] (IMes = 1,3-bis(2,4,6-trimethylphenyl)-imidazolin-2-ylidene); [Co] = Cp‴Co (Cp‴ = $C_5H_2tBu_3$), R = CH_2SiMe_3, *t*Bu; Ar* = 2,6-dibenzhydryl-4-isopropylphenyl; (c) [LCo] = (Ar*BIAN)Co, R = Cy, Ph.

fragmentation process, releasing a monophosphorus species in the form of an acylcyanophosphide.

Our previous work has revealed that polyphosphido complexes exhibit promising reactivity toward electrophiles and nucleophiles, indicating that transition-metal-P_n complexes hold potential as precursors for the targeted synthesis of unique (poly-)phosphorus compounds (Figure 1).[5,8] Building upon these insights, we herein report the functionalization of the anionic complex $\mathbf{1}^-$ and its acylated, neutral counterpart **2** with electrophilic heterocumulenes. In this study, we present the synthesis of anionic cobalt complexes $\mathbf{3}^-$ and $\mathbf{4}^-$, featuring $CoP_4CS_2^-$ and $Co(\eta^3{:}\eta^1\text{-}P_4SN_2(SiMe_3)_2)^-$ cores, respectively. We investigate their structural and electronic properties, as revealed by X-ray crystallography using synchrotron radiation and density functional theory (DFT). Additionally, the reactivity of complexes $\mathbf{3}^-$ and $\mathbf{4}^-$ toward electrophiles in salt metathesis is examined. We also demonstrate the feasibility of further functionalizing the polyphosphido ligand in $CoP_4C(O)tBu$ with isothiocyanates, resulting in the formation of $[Co(\eta^3{:}\eta^1\text{-}P_4C(S)N(R)C(O)tBu)]$ complexes (**6**, R = Cy, Ph).

RESULTS AND DISCUSSION

The addition of carbon disulfide to a purple solution of [K(18c-6)]**1** in THF resulted in a blue coloration within a few hours. $^{31}P\{^1H\}$ NMR spectroscopy confirmed the complete conversion of anionic $\mathbf{1}^-$ into a single new species, [K(18c-6)][(Ar*BIAN)-$Co(\eta^3{:}\eta^1\text{-}P_4CS_2)$] ([K(18c-6)]**3**), exhibiting an AXY_2 spin system (vide infra). This new complex crystallized in 89% yield as dark blue blocks from a THF/*n*-hexane mixture (Scheme 1).

Scheme 1. Addition of CS_2 to the Tetraphosphido Ligand in [K(18c-6)]1[a]

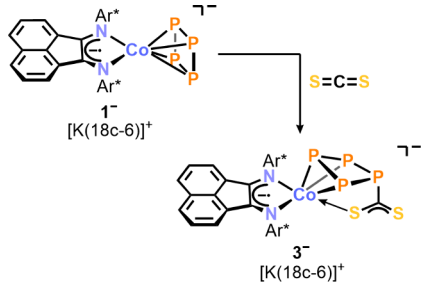

[a]Reagents and conditions: 1.2 equiv of CS_2; THF, r.t., 1 d; yield: [K(18c-6)]**3**: 89%.

Single crystal X-ray diffraction (SCXRD) analysis elucidated the structure of the complex, revealing a puckered *cyclo*-P_4 ligand in a η^3-coordinating mode (Figure 2a). A CS_2 moiety is bound via the carbon atom to the noncoordinating phosphorus atom P4. Additionally, one sulfur atom from the CS_2 moiety exhibits η^1-coordination to the cobalt center. The similar C−S bond distances, 1.698(5) Å and 1.664(5) Å, are intermediate between those of typical C−S single and double bonds ($\sum r_{CS}$ 1.78 Å vs 1.61 Å).[9] The Co−S1 bond length (2.2724(1) Å) is notably longer than the Co−S distance in the structurally related complex [(triphos)Co(η^2-CS_2)] (2.206(4) Å; triphos = MeC-$(CH_2PPh_2)_3$) and exceeds the length of a typical Co−S single bond ($\sum r_{CoS}$ 2.14 Å).[10] These observations support the description of the P_4CS_2 ligand as featuring a delocalized exocyclic CS_2-moiety acting as a pendant donor ligand, as depicted in Scheme 1. The delocalization of the η^3-coordinated P1−P2−P3 moiety is apparent by shorter bond lengths among the coordinating phosphorus atoms (P1−P2 2.169(2) Å and P2−P3 2.169(7) Å) compared to those involving the non-coordinating ones (P1−P4 2.228(6) Å and P3−P4 2.222(7) Å). This structural motif is similar to the behavior observed in the related complex [(Ar*BIAN)Co($\eta^3{:}\eta^1$-$P_4C(O)tBu$)] (**2**, vide infra) and in the series of complexes [Cp‴Co(η^3-P_4R_2)] (R = Ph, Cy, *t*Bu).[7,11]

The $^{31}P\{^1H\}$ NMR spectrum of [K(18c-6)]**3** features an AXY_2 spin system, corroborating the existence of a C_s symmetric tetraphosphido ligand (Figure 2b). The simulated P−P coupling constants are in agreement with those of [Cp‴Co(η^3-P_4R_2)] complexes, reported to exhibit AMM′X spin systems, and the previously reported complex **2**, which gives rise to an AM_2X spin system.[7,11] The resonance for the coordinating phosphorus atom P_x at δ = 99.6 ppm is shifted significantly upfield in comparison to **2** (δ = 323.3 ppm) but appears downfield shifted relative to the equivalent phosphorus atom of [Cp‴Co(η^3-P_4Ph_2)] (δ = −80.7 ppm).

Inspired by the successful functionalization of the *cyclo*-P_4 ligand in $\mathbf{1}^-$ with CS_2 (vide supra), we extended our investigation to include reactions with other heterocumulenes. While attempts to functionalize the P_n moieties with isocyanates and isothiocyanates led to complex mixtures of products that impeded characterization, the use of sulfur diimide $S(NSiMe_3)_2$ resulted in the selective formation of [K(18c-6)][(Ar*BIAN)-$Co(\eta^3{:}\eta^1\text{-}P_4SN_2(SiMe_3)_2)$] ([K(18c-6)]**4**, Scheme 2a). $^{31}P\{^1H\}$ NMR spectroscopic monitoring revealed a quantitative reaction and complete conversion within 6 days at 35 °C, using a slight excess of the diimide (1.5 equiv). Surprisingly, the diimide variant with alkyl substituents, $S(NtBu)_2$, did not undergo any

https://doi.org/10.1021/acs.inorgchem.4c00808
Inorg. Chem. XXXX, XXX, XXX−XXX

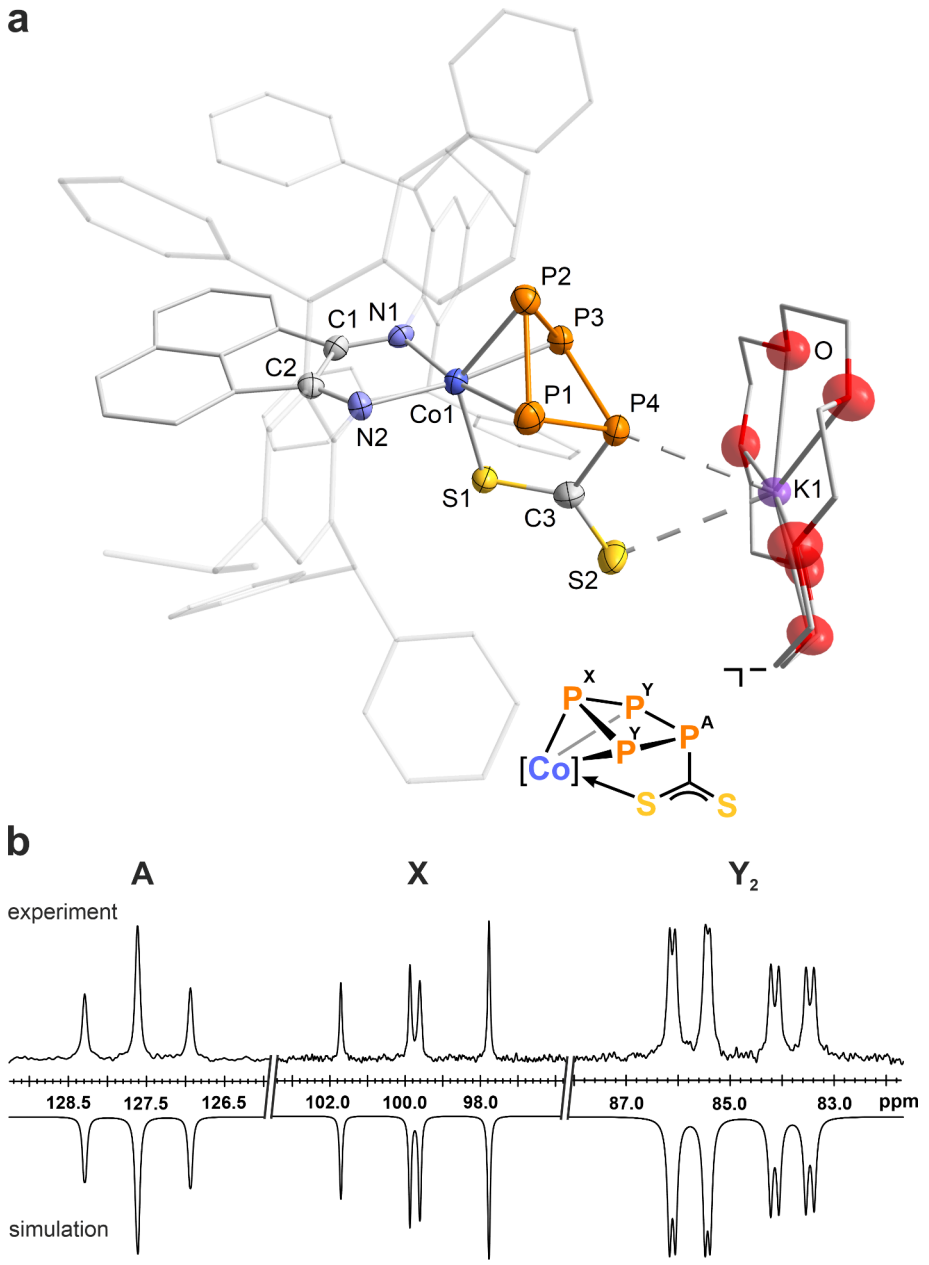

Figure 2. (a) Solid-state molecular structure of [K(18c-6)][(Ar*BIAN)Co(η^3:η^1-P_4CS_2)] ([K(18c-6)]**3**); thermal ellipsoids are shown at the 50% probability level; hydrogen atoms, solvent molecules, and disorder are omitted for clarity. Selected bond lengths [Å] and angles [deg]: P1−P2 2.169(2), P2−P3 2.1697(2), P3−P4 2.230(2), P1−P4 2.2286(2), Co1−P1 2.2936(1), Co1−P2 2.3031(2), Co1−P3 2.2815(2), Co1−S1 2.2725(1), Co1−N1 1.998(4), Co1−N2 1.976(4), P4−C3 1.850(6), C3−S1 1.698(5), C3−S2 1.664(5), P1−P2−P3 85.08(7), P2−P3−P4 88.93(7), P3−P4−P1 82.44(6), P4−P1−P2 88.81(8). (b) Experimental (upward) and simulated (downward) $^{31}P\{^1H\}$ NMR spectra of [K(18c-6)]**3** in THF-d_8 with nuclei assigned to an AXY_2 spin system: $\delta(P_A)$ = 127.6 ppm, $\delta(P_X)$ = 99.6 ppm, $\delta(P_Y)$ = 84.9 ppm, $^1J_{XY}$ = −320 Hz, $^1J_{AY}$ = −110 Hz, $^2J_{AX}$ = 5 Hz.

Scheme 2. Reaction of [K(18c-6)]1 with Sulfur Diimide and Subsequent Functionalization with Trimethylsilyl Chloride[a]

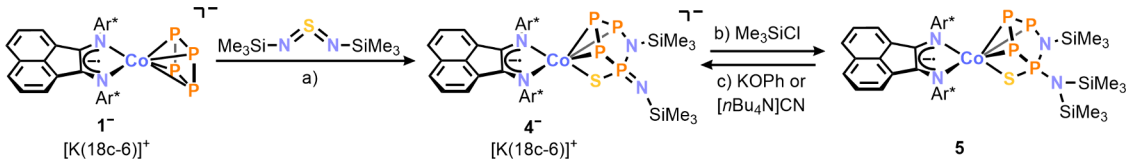

[a]Reagents/byproducts and conditions: (a) 1.5 equiv of $S(NSiMe_3)_2$; THF, 35 °C, 6 d; (b) Me_3SiCl/ −[K(18c-6)]Cl; toluene, r.t., 3 h; (c) 1.0 equiv of [nBu$_4$N]CN; C_6D_6, r.t., 3 h or 1.0 equiv of KOPh/1.0 equiv of 18c-6; C_6D_6, r.t., 3 d; yields [K(18c-6)]**4**: 63%, **5**: 63%.

reaction under similar conditions, or at further elevated temperature.

A SCXRD analysis, using synchrotron radiation at the Rossendorf Beamline BM20 (ESRF), conducted on crystals

https://doi.org/10.1021/acs.inorgchem.4c00808
Inorg. Chem. XXXX, XXX, XXX−XXX

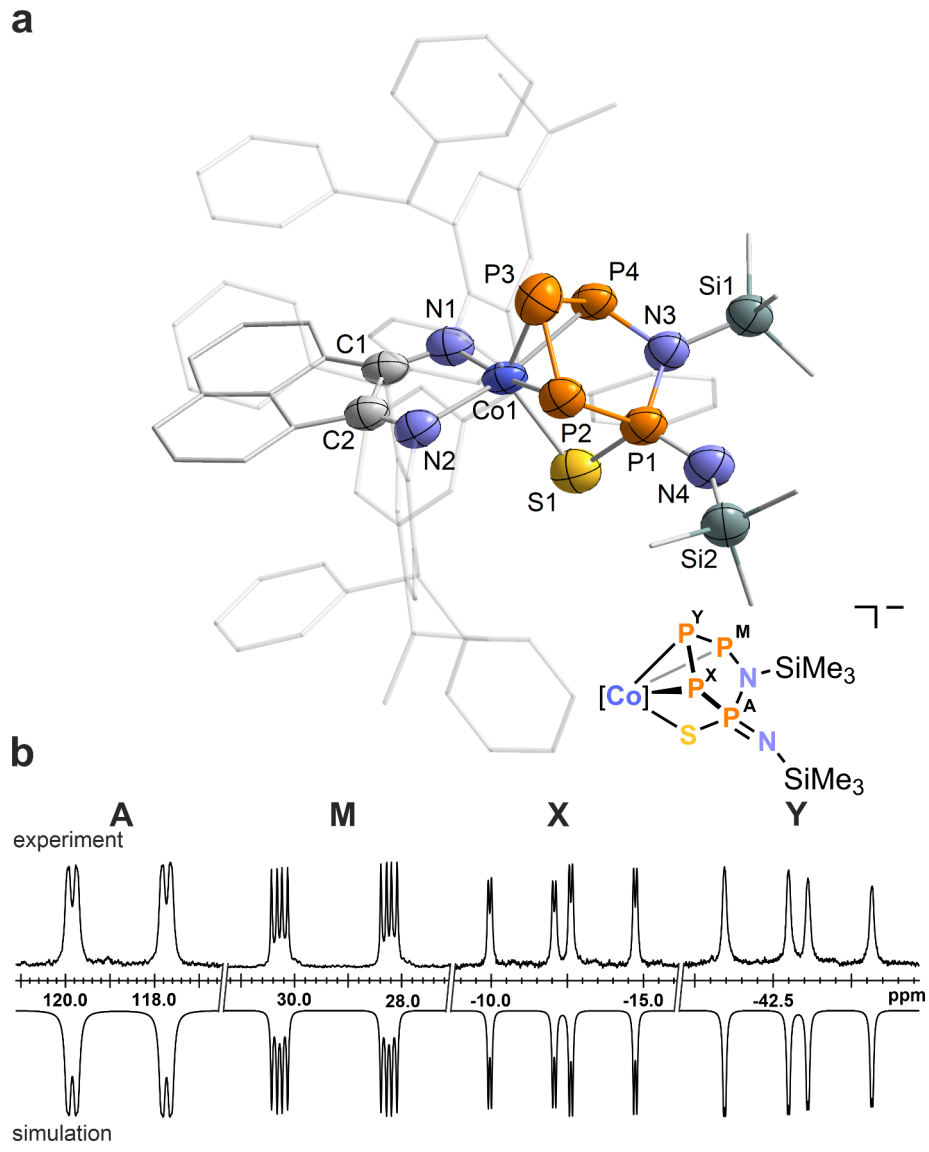

Figure 3. (a) Solid-state molecular structure of [K(18c-6)][(Ar*BIAN)Co(η^3:η^1-$P_4SN_2(SiMe_3)_2$)] ([K(18c-6)]**4**); thermal ellipsoids are shown at the 50% probability level; hydrogen atoms, solvent molecules, $[K(18c\text{-}6)]^+$, and disorder are omitted for clarity. Selected bond lengths [Å] and angles [deg]: P1−P2 2.205(2), P2−P3 2.047(2), P3−P4 2.200(8), P1−N3 1.681(4), P4−N3 1.749(5), P1−S1 2.049(2), P1−N4 1.567(5), Co1−P2 2.336(2), Co1−P3 2.235(2), Co1−P4 2.327(2), Co1−S1 2.391(2), P1−P2−P3 103.00(7), P2−P3−P4 95.57(8), P3−P4−N3 104.75(2), P4−N3−P1 109.5(3), Co1−S1−P1 81.90(8), Si1−N3−P1 124.6(3), Si2−N4−P1 134.0(3). (b) Experimental (upward) and simulated (downward) $^{31}P\{^1H\}$ NMR spectra of **4**$^-$ with nuclei assigned to an AMXY spin system: $\delta(P_A)$ = 118.8 ppm, $\delta(P_M)$ = 29.2 ppm, $\delta(P_X)$ = −12.4 ppm, $\delta(P_Y)$ = −43.2 ppm, $^1J_{XY}$ = −431 Hz, $^1J_{AX}$ = −343 Hz, $^1J_{MY}$ = −331 Hz, J_{MX} = 17 Hz, J_{AY} = 10 Hz, J_{AM} = −32 Hz.

obtained from a toluene/*n*-hexane mixture, revealed the structure of anion **4**$^-$, featuring an η^3-coordinating azatetraphosphole ring (Figure 3a).[12] The structure bears an exocyclic $NSiMe_3$ group alongside a sulfur atom, both bound to the same phosphorus atom, indicating the insertion of a Me_3SiN moiety into a P−P bond. The azaphosphole ring adopts an envelope conformation with the nitrogen atom N3 positioned at the apex, at a distance of 0.700(6) Å above the plane formed by P1, P2, P3, and P4. This conformation resembles cyclic P_4N frameworks observed in oligophosphines such as *cyclo*-$[NP(PPh_2)_2]_2$, *cyclo*-$[(PMe)(PPh_2)N]_2$, and *cyclo*-$[(PPh)_4NR]$ (R = Me, Cy),[13d,h] as well as related compounds.[13] To our knowledge, [K(18c-6)]**4** is the first example of a transition metal complex bearing a *cyclo*-P_4N ligand framework. The P1−P2 and the P3−P4 bond lengths of 2.205(2) Å and 2.200(8) Å, respectively, agree with typical P−P single bonds ($\sum r_{PP}$ 2.22 Å), whereas the P2−P3 bond length at 2.047(2) Å suggests partial P═P double bond character.[9] This interpretation is supported by calculated bond orders of 0.89, 1.05, and 1.13, despite the optimized P2−P3 distance in the theoretical models (2.155 Å) being slightly longer than the experimental value (vide infra).

To corroborate the molecular structure derived from SCXRD data, we carried out geometry optimization for anion **4**$^-$ using the TPSS-D4/def2-TZVP CPCM level of theory. Subsequent intrinsic bond orbital analysis (IBO, see SI for details) identified single bonds within the cyclic P_4N moiety and a polarized P═N (P1−N4) double bond (see IBO 155 in Figure S43 in SI).[14] Additionally, a lone pair was observed on N4, residing in a p-type orbital with slight delocalization over the P_2N unit, which contributes to the stabilization of the planar geometry at N4. The Mayer bond order (MBO) analysis further supports the double bond character of the P1−N4 bond, with a calculated

https://doi.org/10.1021/acs.inorgchem.4c00808
Inorg. Chem. XXXX, XXX, XXX−XXX

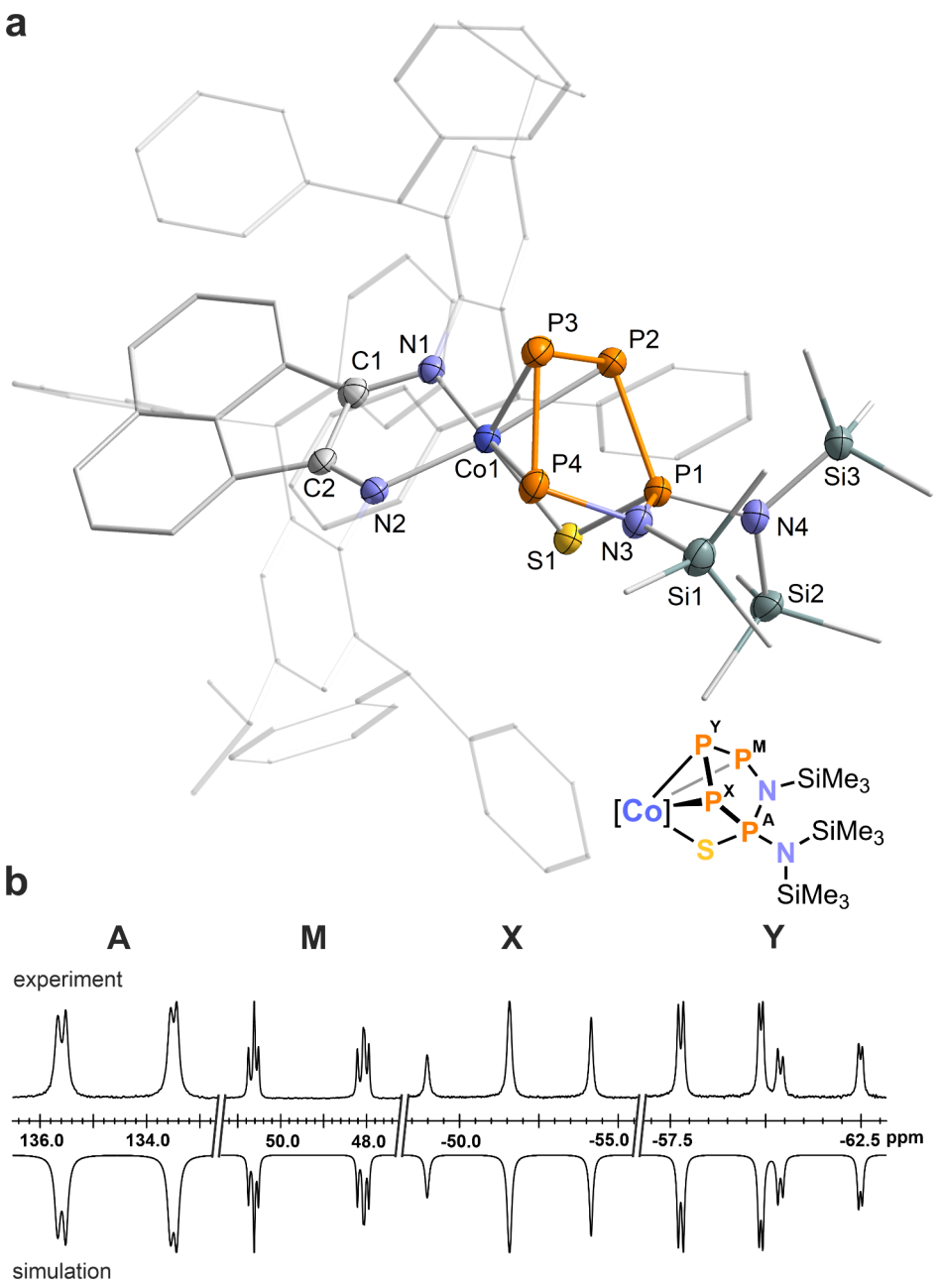

Figure 4. (a) Solid-state molecular structure of [(Ar*BIAN)Co(η^3:η^1-$P_4SN_2(SiMe_3)_3$)] (**5**); thermal ellipsoids are shown at the 50% probability level; hydrogen atoms, solvent molecules and disorder are omitted for clarity. Selected bond lengths [Å] and angles [deg]: P1−P2 2.1966(2), P2−P3 2.1451(2), P3−P4 2.1789(2), Co1−P2 2.3297(1), Co1−P3 2.3210(1), Co1−P4 2.2935(1), Co1−S1 2.3416(1), Co1−N1 1.970(4), Co1−N2 1.986(3), P1−N3 1.670(4), P4−N3 1.782(4), P1−N4 1.666(4), P1−S1 2.0261(2), P1−P2−P3 100.50(6), P2−P3−P4 94.04(6), P2−P1−N4 120.79(1), P1−N3−P4 106.3(2), P1−N4−Si3 120.1(2), Si3−N4−Si2 120.8(2). (b) Experimental (upward) and simulated (downward) $^{31}P\{^1H\}$ NMR spectra of **5** with nuclei assigned to an AMXY spin system: $\delta(P_A)$ = 134.5 ppm, $\delta(P_M)$ = 49.3 ppm, $\delta(P_X)$ = −51.8 ppm, $\delta(P_Y)$ = −59.9 ppm, $^1J_{XY}$ = −423 Hz, $^1J_{MY}$ = −425 Hz, $^1J_{AX}$ = −350 Hz, J_{MX} = 31 Hz, J_{AY} = 11 Hz, J_{AM} = −21 Hz.

MBO of 1.57. These theoretical insights align well with the P1−N4 bond length of 1.567(5) Å, which falls in the expected range for a P═N double bond ($\sum r_{PN}$ 1.62 Å).[9] Conversely, the MBO value of the endocyclic P1−N3 and P4−N3 bonds are 1.05 and 0.95, respectively, indicative of single bonds.

The $^{31}P\{^1H\}$ NMR spectrum of [K(18c-6)]**4** in CD_3CN exhibits an AMXY spin system, distinguished by large $^1J_{PP}$ coupling constants ranging from −331 Hz to −431 Hz, with chemical shifts recorded at δ = 118.8 (P_A), 29.2 (P_E), −12.4 (P_M), and −43.2 (P_X) ppm (Figure 3b and Figure S7, SI). These findings are characteristic for an asymmetric *catena*-P_4 unit, consistent with previous observations for similar systems.[7,8b,15] The assignment of the resonances is based on the assumption that the tetrasubstituted P_1 atom gives rise to the most deshielded ^{31}P NMR signals. The largest $^1J_{PP}$ coupling constant was observed between phosphorus atoms P2 and P3, further supporting partial P═P double bond character. In the $^{29}Si\{^1H\}$ NMR spectrum, two distinct doublets emerge: one at δ = −17.9 ppm corresponding to the imino group, and one at δ = 3.6 ppm, assigned to the amino group. These groups feature $^2J_{SiP}$ coupling constants of 16.6 and 6.1 Hz, respectively. For comparison, the resonance of $S(NSiMe_3)_2$ appears at δ = 1.6 ppm in $C_6D_5CD_3$.[16]

https://doi.org/10.1021/acs.inorgchem.4c00808
Inorg. Chem. XXXX, XXX, XXX−XXX

The more pronounced $^{2}J_{SiP}$ coupling associated with the exocyclic $NSiMe_3$ group is likely a consequence of its involvement in the P1═N4 multiple bond.

Given the ionic nature of $\mathbf{4}^-$ and the anticipated nucleophilicity of the phosphaimino nitrogen N4 (Mulliken charge −0.48), we hypothesized that it would readily undergo salt metathesis reactions with electrophiles. Our assumption was confirmed when the addition of Me_3SiCl to a solution of [K(18c-6)]**4** in toluene resulted in an immediate color change from blue to purple due to the formation of [(Ar*BIAN)Co-(η^3:η^1-$P_4SN_2(SiMe_3)_3$)] (**5**, Scheme 2b), which was crystallized as purple needles from *n*-hexane at −35 °C in 63% isolated yield. Synchrotron SCXRD analysis of **5** revealed the silylation of the imino moiety, resulting in a bis(trimethylsilyl)amino group (Figure 4a).[12] The structural characteristics of **5** closely resemble those of its precursor $\mathbf{4}^-$ (vide supra), including the presence of a central η^3-coordinating azatetraphosphole ring. However, the P1−N4 bond length (1.666(4) Å) is elongated due to its increased single bond character. The silylated nitrogen atom N4 in **5** adopts an almost trigonal planar geometry ($\sum\angle$ 358°) positioned 0.144(4) Å above the plane defined by Si2, Si3, and the chiral phosphorus atom P1. The presence of the trimethylsilyl groups attached to N4 is reflected in the ^{1}H NMR spectrum by two distinct signals, which persist even when the sample is subjected to variable temperature (VT) NMR experiments at up to 100 °C (Figure S11, SI).

This phenomenon is attributed to restricted rotation around the P1−N4 bond, which frustrates chemical equivalence of the trimethylsilyl groups on the NMR time scale. In addition, the three inequivalent silicon atoms are discernible in the ^{29}Si{^{1}H} NMR spectrum, giving rise to two doublets at δ = 7.4 (Si3, $^{2}J_{SiP}$ = 11 Hz) and δ = 11.6 ppm (Si2, $^{2}J_{SiP}$ = 6 Hz), as well as a singlet at δ = 9.3 ppm for Si1. The assignment of the signals has been facilitated through both homo- and heteronuclear 2D NMR spectroscopy, further supported by the observed $^{2}J_{SiP}$ coupling constants (vide supra). The P_4 unit in **5** gives rise to an AMXY spin system in the ^{31}P{^{1}H} NMR spectrum (Figure 4b), featuring chemical shifts and coupling constants akin to those of the precursor $\mathbf{4}^-$ and related asymmetric P_4-chains.[7,8b,15] In contrast, the symmetrical, uncoordinated, and cyclic azaphosphane [$(PPh)_4NMe$] exhibits two multiplet resonances at δ = 126.0 ppm and δ = 13.2 ppm, which are distinct from the resonances of compound **5**.[13h] In particular, the resonances of the middle phosphorus atoms in the chain of **5** are observed at higher field at δ = −51.8 ppm and δ = −59.9 ppm.

The addition of the $SiMe_3$ group is a reversible process, as treatment of **5** with either cyanide or alkoxide salts regenerate anion $\mathbf{4}^-$. These feature either $[n\mathrm{Bu_4N}]^+$ or $[\mathrm{K(18c\text{-}6)}]^+$ cations, depending on the salt used (Scheme 2c), resembling classic acid−base reactivity (Figure S27).

Shifting our focus from anionic *cyclo*-P_4 complex $\mathbf{1}^-$, we investigated the acylated and neutral [(Ar*BIAN)Co(η^3:η^1-$P_4C(O)t\mathrm{Bu}$)] (**2**), anticipating it might exhibit similar reactivity toward electrophilic heterocumulenes. However, likely due to the reduced nucleophilicity of the acylated phosphorus atoms in **2**, no significant reactivity was observed with either CS_2 or $S(NR)_2$. Nonetheless, the addition of sulfur-containing isothiocyanates, specifically CyNCS or PhNCS, to a solution of **2** resulted in a notable color change from magenta to purple (Scheme 3). The reaction with PhNCS (1.1 equiv) led to the complete conversion of **2** within 3 h, according to ^{31}P{^{1}H} NMR spectroscopic monitoring. In contrast, the reaction with CyNCS (1.4 equiv) proceeded at a markedly slower pace and achieved

Scheme 3. Insertion of Isothiocyanates into the P−C Bond of 2[a]

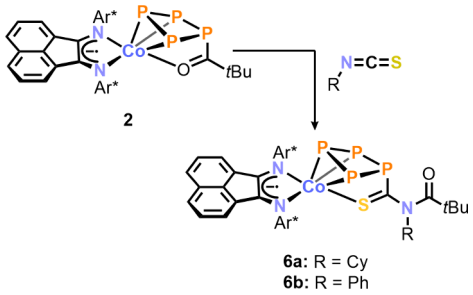

[a]Reagents and conditions: 1.4 equiv of CyNCS; toluene, r.t., 3 d (**6a**); 1.1 equiv of PhNCS; toluene, r.t., 3 h (**6b**); yields **6a**: 80% **6b**: 63%.

full conversion after 3 days. We propose a reaction mechanism for the isothiocyanate insertion that begins with the attack of the acylated phosphorus atom on the carbon atom of the heterocumulene. This is followed by attack of the nitrogen on the carbonyl carbon atom and finally the coordination of the sulfur atom to the cobalt center (see the SI, Scheme S2). The resulting complexes [(Ar*BIAN)Co(η^3:η^1-$P_4C(S)N(R)C(O)t\mathrm{Bu}$)] (R = Cy (**6a**); R = Ph (**6b**)) were isolated in 80% and 64% yield, respectively.

Single-crystal XRD analysis performed on large block-shaped crystals, grown from toluene, confirmed the insertion of the isothiocyanate into the P−C bond of **2**, forming **6a** (Figure 5). While there are documented instances of isothiocyanates undergoing insertion into P−P, P−Si, and P−H bonds, to our knowledge this marks the first example of such a reaction involving a P−C bond.[5,17] In **6a**, the thioacyl group coordinates

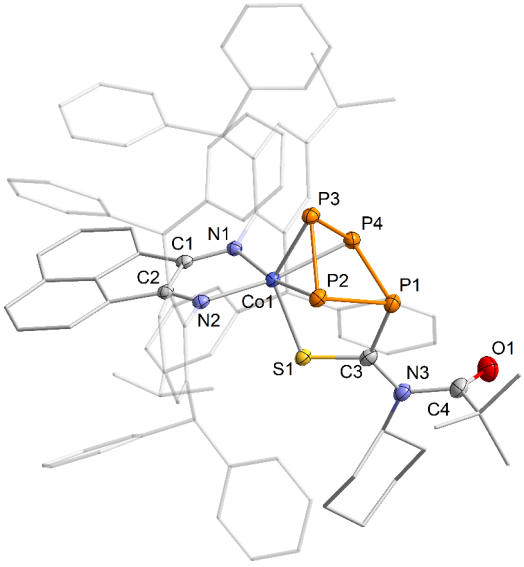

Figure 5. Solid-state molecular structure of [(Ar*BIAN)Co(η^3:η^1-$P_4C(S)N(Cy)C(O)t\mathrm{Bu}$)] (**6a**); thermal ellipsoids are shown at the 50% probability level; hydrogen atoms and solvent molecules are omitted for clarity. Selected bond lengths [Å] and angles [deg]: P1−P2 2.2437(8), P2−P3 2.1697(7), P3−P4 2.1669(8), P1−P4 2.2360(7), Co1−P2 2.2881(5), Co1−P3 2.2915(6), Co1−P4 2.2838(8), Co1−S1 2.2583(6), Co1−N1 1.9701(2), Co1−N2 1.9693(2), S1−C3 1.696(2), C3−N3 1.343(3), C4−N3 1.471(3), P1−C3 1.856(2), C4−O1 1.196(3), P1−P2−P3 88.80(3), P2−P3−P4 85.38(3), P3−P4−P1 89.07(3), P4−P1−P2 82.05(3).

https://doi.org/10.1021/acs.inorgchem.4c00808
Inorg. Chem. XXXX, XXX, XXX−XXX

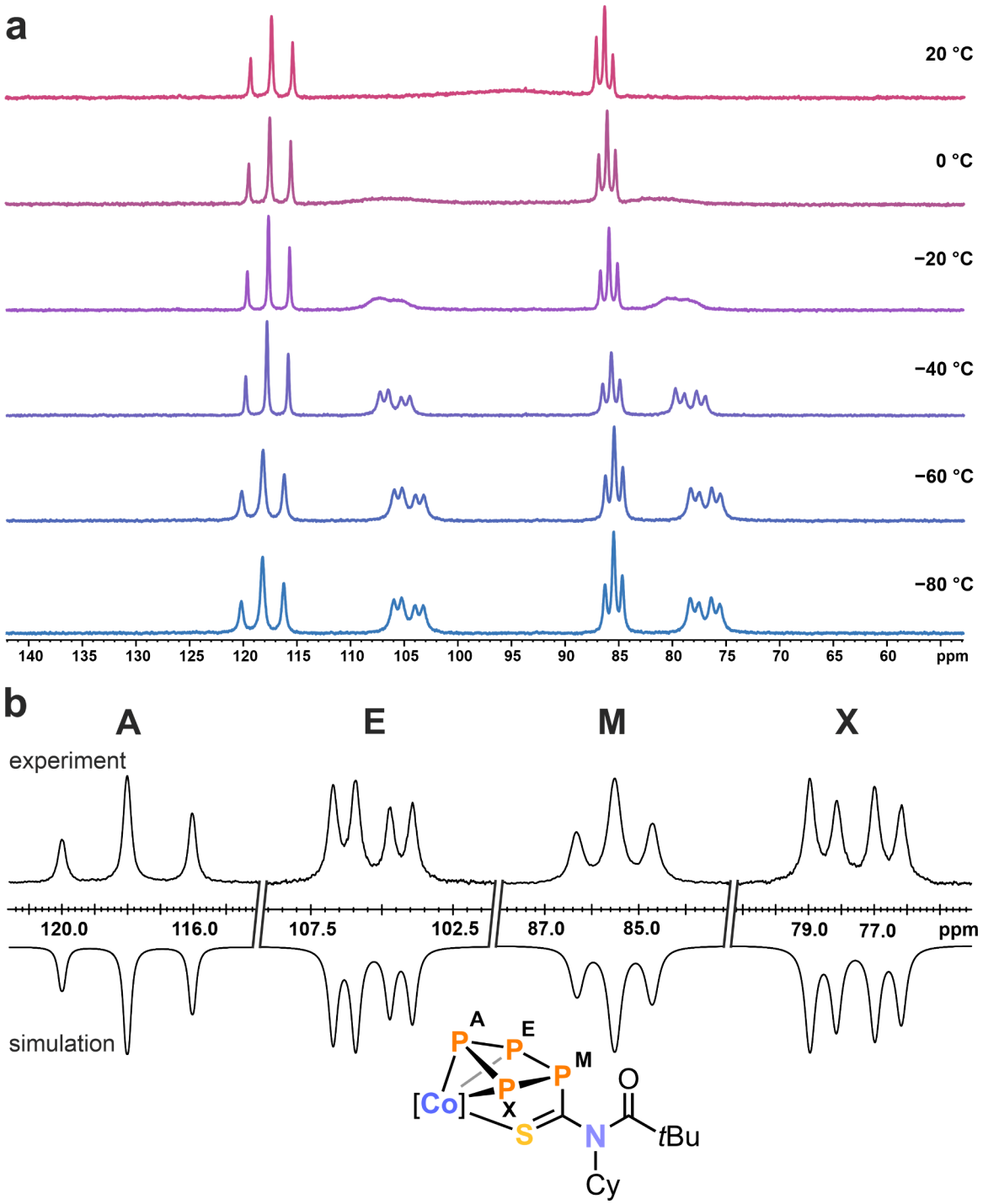

Figure 6. (a) Variable temperature $^{31}P\{^{1}H\}$ NMR spectra of **6a** in toluene-d_8. (b) Experimental (upward) and simulated (downward) $^{31}P\{^{1}H\}$ NMR spectra of **6a** at −60 °C in toluene-d_8 with nuclei assigned to an AEMX spin system: $\delta(P_A)$ = 117.9 ppm, $\delta(P_E)$ = 105.4 ppm, $\delta(P_M)$ = 85.5 ppm, $\delta(P_X)$ = 77.6 ppm, $^{1}J_{AE}$ = −324 Hz, $^{1}J_{AX}$ = −321, $^{1}J_{EM}$ = −129 Hz, $^{1}J_{MX}$ = −133 Hz, $^{2}J_{AM}$ = 18 Hz, $^{2}J_{EX}$ = 20 Hz.

to the cobalt via the sulfur atom, rather than through the oxygen atom of the remote acyl group.[7] This coordination shift is reflected in the ATR-IR spectrum, where the C═O stretching vibration in **6a** was distinctly observed at $\tilde{\nu}_{CO}$ = 1727 cm^{-1}, a band typical for acyl groups.[18] This contrasts the C═O stretch in **2**, which was predicted to occur at $\tilde{\nu}_{CO}$ = 1462 cm^{-1}, thereby overlapping with the BIAN C−N vibrations in the fingerprint region.[7] The puckered *cyclo*-P_4 moiety observed in complex **6a** closely resembles that in complexes **2**, **3**$^{-}$ and [Cp‴Co(η^3-P_4R_2)] (Cp‴ = $C_5H_2tBu_3$; R = Ph, Cy, *t*Bu),[7,11] featuring elongated P1−P2 (2.2437(8) Å) and P1−P4 (2.2360(7) Å) bond lengths alongside shorter P2−P3 (2.1697(7) Å) and P3−P4 (2.1669(8) Å) bond lengths, indicative of some degree of multiple bond character. Furthermore, the bond lengths of S1−C3 (1.696(2) Å) and C3−N3 (1.343(3) Å) are elongated relative to those in free aryl isothiocyanate (S−C, 1.566 Å; C−N 1.152 Å), indicating increased single bond character in **6a**.[19] The coordination sphere of the cobalt center is completed by an Ar*BIAN$^{\bullet-}$ radical anion.[20] The phenyl-substituted derivative is essentially isostructural with **6b** (Figure S41, SI).

https://doi.org/10.1021/acs.inorgchem.4c00808
Inorg. Chem. XXXX, XXX, XXX−XXX

The $^{31}P\{^{1}H\}$ NMR spectrum of **6a** in C_6D_6 features two triplets at $\delta = 86.3$ (P_M) ppm and $\delta = 117.3$ (P_A) ppm, as well as a significantly broadened signal ($\Delta\nu_{1/2} = 2500$ Hz) at $\delta = 93.0$ ($P_{E/X}$) ppm. This broadening suggests a dynamic process occurring in solution. Given the solid-state molecular structure of **6a**, two distinct signals are expected for the phosphorus atoms P2 and P4 if the rotation is restricted around the C4−N3 or the C3−N3 axis, with the latter axis exhibiting partial multiple bond character (1.343(3) Å vs $\sum r_{CN}$ 1.46 Å for a single bond; labeling according to Figure 5). VT $^{31}P\{^{1}H\}$ NMR spectroscopy elucidated this phenomenon further, revealing that the broad resonance at ambient temperature separates into two distinct signals at 0 °C. These resolve below −40 °C into distinct multiplets, indicative of an AEMX spin system (Figure 6). In contrast, the $^{31}P\{^{1}H\}$ NMR spectrum of **6b**, which possesses nearly identical C3−N3 and C4−N3 bond lengths, displays well-resolved signals conforming to an AB_2X spin system with similar chemical shifts akin to those of **6a** (see Figure S23, SI). This distinct behavior in solution is probably due to hindered rotation resulting from the steric demand of the substituent.

CONCLUSION

The reaction of anionic *cyclo*-P_4 complex $\mathbf{1}^-$ with CS_2 leads to the electrophilic addition of the heterocumulene to the *cyclo*-P_4 ligand, resulting in the formation of $\mathbf{3}^-$, which features a puckered $\eta^3{:}\eta^1$-P_4CS_2 ligand. Initial reactivity studies of $\mathbf{3}^-$ toward electrophiles indicate a propensity for salt metathesis reactions, suggesting new pathways for subsequent functionalization. Upon employing the sulfur diimide $S(NSiMe_3)_2$ as the reactant, P−P bond insertion was facilitated for *cyclo*-P_4 complex $\mathbf{1}^-$, yielding complex $\mathbf{4}^-$, with a novel CoP_4N^- core. Compound $\mathbf{3}^-$ represents the first azatetraphosphole complex and undergoes further functionalization to yield **5** upon reaction with Me_3SiCl. These compounds, $\mathbf{4}^-$ and **5**, have been characterized with various analytical techniques, including single crystal X-ray structural analysis at synchrotron facilities and computational chemistry studies. The neutral complex **2** exhibits discrepant reactivity, undergoing insertion of isothiocyanates into the P−C bond of the acylated tetraphosphido ligand, yielding the highly derivatized complexes **6a** and **6b**. This new reaction type expands the repertoire of P−C bond insertion reactions available for the strategic functionalization of tetraphosphido ligands.

Overall, our findings highlight the versatility and potential of low-valent polyphosphido complexes for effecting targeted and diverse transformations of P_4. With increased availability of routes to various *cyclo*-P_4 complexes, particularly highlighted by recent advancements, this paves the way to unique phosphorus compounds. Ongoing research in this area is instrumental in deepening our understanding of reactivity patterns and mechanisms, laying the essential groundwork for the development of systems capable of facilitating the efficient transition-metal-mediated functionalization of P_4.

EXPERIMENTAL SECTION

General Considerations. All experiments were performed under an atmosphere of dry argon, by using standard Schlenk and glovebox techniques. Solvents were purified, dried, and degassed with an MBraun SPS800 solvent purification system. All dry solvents except *n*-hexane were stored under argon over activated 3 Å molecular sieves in gastight ampules. *n*-Hexane was stored over a potassium mirror. NMR spectra were recorded on Bruker Avance 400 spectrometers. ^{1}H and $^{13}C\{^{1}H\}$ spectra were referenced internally to residual solvent resonances. $^{31}P\{^{1}H\}$ spectra were referenced externally to 85% H_3PO_4 (aq). The assignment of the ^{1}H and ^{13}C NMR signals was confirmed by two-dimensional (COSY, HSQC, HMBC, NOESY and ROESY) experiments. A more detailed assignment of the signals can be found in the SI. For compounds which give rise to a higher order spin system in the $^{31}P\{^{1}H\}$ NMR spectrum, the resolution enhanced $^{31}P\{^{1}H\}$ NMR spectrum was transferred to the software gNMR, version 5.0.6, by Cherwell Scientific.[21] The full line shape iteration procedure of gNMR was applied to obtain the best match of the fitted to the experimental spectrum. $^{1}J(^{31}P^{31}P)$ coupling constants were set to negative values and all other signs of the coupling constants were obtained accordingly.[22]

UV/vis spectra were recorded on an Ocean Optics Flame Spectrometer with a DH-2000-BAL light source. Elemental analyses were performed by the Central Analytics Department of the University of Regensburg using a Vario micro cube. Mass spectra were recorded on a Finnigan MAT 95 spectrometer. IR spectra were recorded with a Bruker ALPHA spectrometer equipped with a diamond ATR unit.

$S(NSiMe_3)_2$ and CS_2 ($c = 5.0$ M in THF) were purchased from Sigma-Aldrich; PhNCS, CyNCS from Alfa Aesar; and all were used as received. Trimethylsilyl chloride was purchased from Sigma-Aldrich and a stock solution ($c = 1.58$ M in toluene) was prepared. The starting materials [K(18c-6)][(Ar*BIAN)Co(η^4-P_4)] ([K(18c-6)]**1**) and [(Ar*BIAN)Co($\eta^3{:}\eta^1$-$P_4C(O)t$Bu)] (**2**) were prepared according to previously reported procedures.[7]

*[K(18c-6)][(Ar*BIAN)Co($\eta^3{:}\eta^1$-P_4CS_2)] ([K(18c-6)]**3**).* A stock solution of CS_2 (30.6 μL, $c = 5.0$ M in THF, 0.153 mmol, 1.2 equiv) was added to a deep purple solution of [K(18c-6)]**1** (200 mg, 0.128 mmol, 1.0 equiv) in THF (4 mL) at room temperature. The reaction mixture was stirred overnight, resulting in a blue solution which was filtered. The filtrate was layered with *n*-hexane (12 mL). After 3 days, blue shimmering crystals had formed, which were isolated by decantation of the mother liquor, washed with *n*-hexane (2 × 1 mL), and dried in vacuo. The solid contained 0.4 equiv of *n*-hexane and 0.7 equiv of THF after drying as indicated by $^{1}H/^{13}C\{^{1}H\}$ NMR spectra and elemental analysis. Yield: 186 mg (0.115 mmol, 89%). UV/vis: (THF, λ_{max}/nm, ε_{max}/L·mol^{-1}·cm^{-1}): 330 (22 000), 375sh (14 000), 570 (15 000), 725 (10500). ^{1}H NMR (400.13 MHz, 300 K, THF-d_8): δ/ppm = 1.11−1.16 (m, 12H), 2.78 (sept., $^{3}J_{HH} = 6.9$ Hz, 2H), 3.45 (br s, 24H), 5.06 (s, 2H), 5.50 (d, $^{3}J_{HH} = 7.1$ Hz, 2H), 6.22−6.26 (m, 2H), 6.41−6.46 (m, 8H), 6.51−6.59 (m, 4H), 6.65−6.70 (m, 4H), 6.79−6.81 (m, 4H), 6.85−6.86 (m, 2H), 6.90−7.10 (m, 14H), 7.24 (d, $^{3}J_{HH} = 8.2$ Hz, 2H), 7.31−7.33 (m, 4H), 7.57−7.59 (m, 4H), 7.96 (s, 2H). $^{13}C\{^{1}H\}$ NMR (100.66 MHz, 300 K, THF-d_8): δ/ppm = 23.9 (s), 24.3 (s), 34.2 (s), 51.1 (s), 52.5 (s), 71.1 (s), 120.7 (s), 122.9 (s), 125.3 (s), 125.6 (s), 125.7 (s), 125.9 (s), 127.4 (s), 127.5 (s), 127.6 (s), 127.7 (s), 128.0 (s), 128.2 (s), 130.6 (s), 130.8 (s), 130.9 (s), 131.2 (s), 131.5 (s), 134.0 (s), 134.1 (s), 134.4 (s), 138.8 (s), 143.6 (s), 143.9 (s), 145.0 (s), 146.6 (s), 147.6 (s), 150.9 (s), 159.8 (s); *C*=S: not detected. $^{31}P\{^{1}H\}$ NMR (162.04 MHz, 300 K, THF-d_8): δ/ppm = 83.3−86.1 (m, 2P, P_Y), 97.8−101.7 (m, 1P, P_X), 127.6 (t, 1P, P_A), for parameters obtained by simulation, see Figure S3 and Table S1, SI. Anal. Calcd (%) for $(C_{95}H_{92}CoKN_2O_6P_4S_2)\cdot(n\text{-hexane})_{0.4}(THF)_{0.7}$ (M_w = 1643.84 g·mol^{-1}) C 69.62, H 6.02, N 1.62, S 3.71; found C 69.25, H 6.07, N 1.48, S 4.11.

*[K(18c-6)][(Ar*BIAN)Co($\eta^3{:}\eta^1$-$P_4SN_2(SiMe_3)_2$)] [K(18c-6)]**4**).* *N*,*N*-Bis(trimethylsilyl)sulfurdiimide (19.8 mg, 22.6 μL, 0.096 mmol, 1.5 equiv) was added to a deep purple solution of [K(18c-6)]**1** (100 mg, 0.064 mmol, 1.0 equiv) in THF (2 mL). The reaction mixture was stirred at 35 °C for 6 days, resulting in a blue solution which was filtered. *n*-Hexane (40 mL) was added while stirring, precipitating a purple solid, which was isolated by filtration, washed with *n*-hexane (3 × 2 mL), and dried in vacuo. Yield: 71 mg (0.040 mmol, 63%). UV/vis: (THF, λ_{max}/nm, ε_{max}/L·mol^{-1}·cm^{-1}): 320sh (17 000), 550 (10 000), 710 (9000). ^{1}H NMR (400.30 MHz, 300 K, MeCN-d_3): δ/ppm = −0.14 (s, 9H), 0.09 (s, 9H), 1.11−1.17 (m, 12H), 2.76−2.88 (m, 2H), 3.55 (s, 24H), 4.66 (s, 1H), 4.98 (d, $^{3}J_{HH} = 7.1$ Hz, 1H), 5.19 (s, 1H), 5.71 (d, $^{3}J_{HH} = 7.1$ Hz, 1H), 6.06−6.19 (m, 7H), 6.32−6.36 (m, 2H), 6.47−6.59 (m, 7H), 6.73−6.77 (m, 2H), 6.81−6.98 (m, 11H), 7.03−7.32 (m, 16H), 7.43−7.48 (m, 3H), 7.95 (s, 1H), 8.49 (s, 1H). $^{13}C\{^{1}H\}$ NMR (100.61 MHz, 300 K, MeCN-d_3): δ/ppm = 1.5 (d, $^{3}J_{CP} = 3.9$ Hz), 4.7 (d, $^{3}J_{CP} = 3.1$ Hz), 24.2 (s), 24.4 (s), 24.4 (s), 24.6 (s), 34.3 (s), 34.4 (s), 50.9 (s),

https://doi.org/10.1021/acs.inorgchem.4c00808
Inorg. Chem. XXXX, XXX, XXX−XXX

51.3 (s), 51.6 (s), 52.0 (s), 71.0 (s), 120.5 (s), 120.7 (s), 123.0 (s), 123.3 (s), 125.5 (s), 126.0 (s), 126.1 (s), 126.1 (s), 126.2 (s), 126.2 (s), 126.6 (s), 127.5 (s), 127.7 (s), 127.9 (s), 128.1 (s), 128.1 (s), 128.1 (s), 128.2 (s), 128.3 (s), 128.4 (s), 128.7 (s), 128.7 (s), 128.8 (s), 129.3 (s), 130.7 (s), 131.2 (s), 131.2 (s,), 131.3 (s), 131.4 (s), 131.4 (s), 131.6 (s), 131.6 (s), 131.7 (s), 132.9 (s), 134.2 (s), 134.6 (s), 134.7 (s), 134.9 (s), 137.9 (s), 139.3 (s), 143.1 (s), 144.1 (s), 144.4 (s), 144.5 (s), 144.6 (s), 146.7 (s), 147.9 (s), 148.5 (s), 150.0 (s), 153.8 (s), 155.4 (s), 159.9 (s), 161.6 (s). $^{31}P\{^{1}H\}$ NMR (161.98 MHz, 300 K, MeCN-d_3): δ/ppm = −43.2 (dd, 1P, P_Y), − 12.4 (ddd, 1P, P_X), 29.2 (ddd, 1P, P_M), 118.8 (dd, 1P, P_A), for parameters obtained by simulation, see Figure S7 and Table S2, SI. $^{29}Si\{^{1}H\}$ NMR (79.49 MHz, 300 K, MeCN-d_3): δ/ppm = −17.9 (d, $^{2}J_{SiP}$ = 16.6 Hz), 3.6 (d, $^{2}J_{SiP}$ = 6.1 Hz). Anal. Calcd (%) for ($C_{100}H_{110}CoKN_4O_6P_4SSi_2$) (Mw = 1774.15 g·mol^{-1}) C 67.70, H 6.25, N 3.16, S 1.81; found C 67.29, H 6.29, N 3.04, S 1.72. TOF-MS (ESI, MeCN): m/z(%) calcd. for $C_{88}H_{86}CoN_4P_4SSi_2^-$ [M^-]: 1470.4424; found 1470.4298.

*[(Ar*BIAN)Co(η^3:η^1-$P_4SN_2(SiMe_3)_3$)] (**5**).* A stock solution of Me_3SiCl (53.5 μL, 1.58 M in toluene, 0.085 mmol, 1.0 equiv) was added to a blue solution of [K(18c-6)]**4** (150 mg, 0.085 mmol, 1.0 equiv) in toluene (3.5 mL). The reaction mixture was stirred for 3 h, over which the color changed to purple. The suspension was filtered through a pad of silica (0.5 × 1 cm) and washed with toluene (3 × 1 mL). The solvent was removed and the purple residue extracted with *n*-hexane (8 mL). The filtrate was concentrated to half of the original volume. Storage for 1 day at room temperature and 1 day at −35 °C gave numerous shimmering purple crystals, which were isolated by decantation of the mother liquor and dried in vacuo. The crystalline solid contained 0.1 equiv of *n*-hexane and 0.1 equiv of toluene after drying as indicated by $^{1}H/^{13}C\{^{1}H\}$ NMR spectra and elemental analysis. Yield: 82 mg (0.053 mmol, 63%). UV/vis: (THF, λ_{max}/nm, ε_{max}/L·mol^{-1}·cm^{-1}): 330sh (17 000), 550 (11 000), 700 (14 000). ^{1}H NMR (400.13 MHz, 300 K, C_6D_6): δ/ppm = 0.05 (s, 9H), 0.20 (s, 9H), 0.38 (s, 9H), 1.09−1.14 (m, 12H), 2.58−2.71 (m, 2H), 5.40 (s, 1H), 5.43 (s, 1H), 5.55 (d, $^{3}J_{HH}$ = 7.1 Hz, 1H), 6.02 (d, $^{3}J_{HH}$ = 7.1 Hz, 1H), 6.17−6.21 (m, 1H), 6.29−6.33 (m, 1H), 6.49−6.56 (m, 4H), 6.62−6.76 (m, 10H), 6.92−6.94 (m, 2H), 7.03−7.21 (m, 10H, d ($^{3}J_{HH}$ = 8.1 Hz) overlapping with d ($^{3}J_{HH}$ = 8.2 Hz)), 7.27−7.34 (m, 8H), 7.37−7.37 (m, 1H), 7.41−7.44 (m, 7H), 7.46 (s, 1H), 7.51−7.53 (m, 2H), 7.72−7.74 (m, 2H), 7.97 (s). $^{13}C\{^{1}H\}$ NMR (100.61 MHz, 300 K, C_6D_6): δ/ppm = 2.8 (d, $^{3}J_{PC}$ = 8.1 Hz), 5.2 (dd, $^{3}J_{PC}$ = 5.9 Hz, 3.5 H), 5.7 (d, $^{3}J_{PC}$ = 1.8 Hz), 24.0 (s), 24.0 (s), 24.1 (s), 24.1 (s), 33.8 (s), 33.9 (s), 51.1 (s), 51.7 (s), 52.0 (s), 52.4 (s), 121.8 (s), 122.0 (s), 124.4 (s), 124.4 (s), 125.7 (s), 125.9 (s), 126.0 (s), 126.1 (s), 126.2 (s), 127.0 (s), 127.7 (s), 127.7 (s), 127.8 (s), 127.9 (s), 128.0 (s), 128.1 (s), 128.2 (s), 128.3 (s), 128.5 (s), 128.6 (s), 130.2 (s), 130.5 (s), 130.7 (s), 130.8 (s), 130.8 (s), 131.0 (s), 131.0 (s), 131.3 (s), 131.4 (s), 132.3 (s), 132.4 (s), 132.9 (s), 135.2 (s), 136.5 (s), 137.9 (s), 138.8 (s), 142.8 (s), 143.1 (s), 143.4 (s), 143.8 (s), 145.3 (s), 145.5 (s), 146.1 (s), 146.5 (s), 147.8 (s), 148.1 (s), 150.9 (s), 152.2 (s), 163.1 (s), 164.2 (s). $^{31}P\{^{1}H\}$ NMR (162.04 MHz, 300 K, C_6D_6): (AMXY) spin system δ/ppm = −60.1 (dd, 1P, P_Y), −54.2 - −49.0 (m, 1P, P_X), 47.9−50.8 (m, 1P, P_M), 133.4−135.7 (m, 1P, P_A), for parameters obtained by simulation, see Figure S13 and Table S3. $^{29}Si\{^{1}H\}$ NMR (79.49 MHz, 300 K, C_6D_6): δ/ppm = 7.4 (d, $^{2}J_{SiP}$ = 10.9 Hz), 9.3 (s), 11.6 (d, $^{2}J_{SiP}$ = 6.1 Hz). Anal. Calcd (%) for ($C_{91}H_{95}CoN_4P_4SSi_3$)·(toluene)$_{0.1}$·(*n*-hexane)$_{0.1}$ (M_w = 1543.93 g·mol^{-1}) C 70.98, H 6.27, N 3.59, S 2.05; found C 71.33, H 5.88, N 3.51, S 2.07.

*[(Ar*BIAN)Co(η^3:η^1-P_4C(S)N(Cy)C(O)tBu)] (**6a**).* Neat cyclohexyl isothiocyanate (7.3 mg, 7.4 μL, 0.052 mmol, 1.4 equiv) was added to a magenta-colored solution of **2** (50 mg, 0.037 mmol, 1.0 equiv) in toluene (1.5 mL). The reaction mixture was stirred for 3 days, giving a purple solution. The solvent was removed in vacuo. Subsequently, the resulting purple residue was washed with *n*-hexane (3 × 0.5 mL) and dried in vacuo yielding a deep purple powder. Complex **6a** is stable in solution even when heated to 50 °C for up to 3 weeks. Yield: 44 mg (0.030 mmol, 80%). UV/vis: (toluene, λ_{max}/nm, ε_{max}/L·mol^{-1}·cm^{-1}): 330 (12 000), 430 (2500), 550 (5000), 720 (8000). ^{1}H NMR (400.13 MHz, 300 K, C_6D_6): δ/ppm = 0.60−0.65 (m, 5H), 0.92 (s, 9H), 1.02−1.05 (m, 12H), 1.16−1.22 (m, 3H), 1.46−1.49 (m, 2H), 2.58 (sept., $^{3}J_{HH}$ = 6.9 Hz, 2H), 3.43−3.48 (m, 1H), 5.50 (s, 2H), 5.89 (d, $^{3}J_{HH}$ = 7.1 Hz, 2H), 6.22−6.26 (m, 2H), 6.64−6.65 (m, 6H), 6.71−6.75 (m, 2H), 6.82−6.98 (m, 10H), 7.06−7.15 (m, 14H), 7.19 (d, $^{3}J_{HH}$ = 8.2 Hz, 2H), 7.29−7.29 (m, 2H), 7.36−7.37 (m, 2H), 7.35−7.36 (m, 2H), 7.62−7.67 (m, 8H), 7.92 (s, 2H). $^{13}C\{^{1}H\}$ NMR (100.66 MHz, 300 K, C_6D_6): δ/ppm = 24.4 (s), 24.5 (s), 26.1 (s), 26.6 (s), 29.0 (s), 31.2 (s), 34.4 (s), 44.1 (s), 51.7 (s), 53.3 (s), 67.1 (s), 122.6 (s), 125.4 (s), 126.5 (s), 126.6 (s), 126.9 (s), 127.3 (s), 128.4 (s), 128.5 (s), 128.5 (s), 128.7 (s), 129.0 (s), 129.2 (s), 130.6 (s), 130.9 (s), 131.1 (s), 131.4 (s), 132.6 (s), 135.2 (s), 136.8 (s), 139.0 (s), 143.5 (s), 145.3 (s), 146.0 (s), 146.3 (s), 148.5 (s), 149.7 (s), 164.3 (s), 183.1 (s); C═S: not detected. $^{31}P\{^{1}H\}$ NMR (162.04 MHz, 300 K, C_6D_6): δ/ppm = 86.3 (t, 1P, P_M), 93.0 (br s, $\Delta\nu_{1/2}$ = 2500 Hz, 2P, $P_{E/X}$), 117.3 (t, 1P, P_A); (161.98 MHz, toluene-d_8, 213 K): δ/ppm = 77.6 (dd, 1P, P_X), 85.5 (t, 1P, P_M), 105.3 (dd, 1P, P_E), 118.0 (t, 1P, P_A), for parameters obtained by simulation, see Figure S19 and Table S4, SI. IR (solid state): $\tilde{\nu}$/ cm^{-1} = 3058w, 3023w, 2953w, 2928w, 1944w, 1805w, 1727m (C═O), 1600w, 1533m, 1492s, 1446m, 1417m, 1369s, 1322m, 1297m, 1255w, 1193m, 1153w, 1101w, 1076w, 1035m, 1007m, 920w, 895w, 842w, 820m, 761m, 736s, 736m, 696s, 654m, 634m, 606s. Anal. Calcd (%) for ($C_{94}H_{88}CoN_3OP_4S$) (M_w = 1490.65 g·mol^{-1}) C 75.74, H 5.95, N 2.82, S 2.15; found: C 75.60, H 5.93, N 2.58, S 1.75.

*[(Ar*BIAN)Co(η^3:η^1-P_4C(S)N(Ph)C(O)tBu)] (**6b**).* Neat PhNCS (11.0 mg, 9.7 μL, 0.081 mmol, 1.1 equiv) was added to a magenta-colored solution of **2** (100 mg, 0.074 mmol, 1.0 equiv) in toluene (2 mL). The reaction mixture was stirred for 3 h, over which the color changed to purple. The solvent was removed in vacuo, and the purple residue extracted with *n*-hexane (30 mL). The mixture was filtered, and the filtrate concentrated until incipient crystallization. Purple crystals formed upon storage for 2 days at −35 °C. The crude product (84 mg) was isolated by decantation of the supernatant. Recrystallization from Et_2O (2 mL) at −35 °C gave shimmering deep purple crystals, which were isolated by decantation of the mother liquor and dried in vacuo. The compound decomposes to new species (identified by ABMX and AEMX spin systems in the $^{31}P\{^{1}H\}$ NMR spectrum) in solution at ambient temperature over the course of hours. Yield: 69 mg (0.046 mmol, 63%). UV/vis: (toluene, λ_{max}/nm, ε_{max}/L·mol^{-1}·cm^{-1}): 325 (22500), 530 (9000), 710 (13 000). ^{1}H NMR (400.13 MHz, 300 K, C_6D_6,): δ/ppm = 0.76 (s, 9H), 1.00−1.03 (m, 12H), 2.55 (sept., $^{3}J_{HH}$ = 6.9 Hz, 2H), 5.45 (s, 2H), 5.80−5.82 (m, 2H), 5.85 (d, $^{3}J_{HH}$ = 7.1 Hz), 6.21−6.25 (m, 2H), 6.57−6.82 (m, 17H), 7.01−7.16 (m, 16H), 7.25−7.29 (m, 6H), 7.31−7.34 (m, 6H), 7.57 (s, 2H), 7.74−7.76 (br m, 4H). $^{13}C\{^{1}H\}$ NMR (100.61 MHz, 273 K, toluene-d_8): δ/ppm = 24.3 (s), 24.5 (s), 28.5 (s), 34.3 (s), 43.3 (s), 51.4 (s), 52.9 (s), 122.5 (s), 125.5 (s), 126.5 (s), 126.5 (s), 126.6 (s), 127.2 (s), 127.9 (s), 128.3 (s), 128.3 (s), 128.4 (s), 128.5 (s), 128.6 (s), 128.8 (s), 128.7 (s), 128.9 (s), 130.1 (s), 130.2 (s), 130.7 (s), 130.9 (s), 131.1 (s), 132.0 (s), 135.2 (s), 136.6 (s), 138.7 (s) 141.6 (s), 142.7 (s), 145.0 (s), 145.8 (s), 146.2 (s), 148.5 (s), 149.0 (s), 164.4 (s), 182.2 (s); C═S: not detected. $^{31}P\{^{1}H\}$ NMR (162.04 MHz, 300 K, C_6D_6): (AB_2X) spin system δ/ppm = 95.5−98.8 (m, 1P, P_x), 103.8−109.5 (m, 3P, P_A/P_B), for parameters obtained by simulation, see Figure S23 and Table S5. IR (solid state): $\tilde{\nu}$/ cm^{-1} = 3056w, 3023w, 2956w, 2924w, 2160w, 2031w, 1735w (C═O), 1685w, 1598w, 1530w, 1492m, 1450m, 1471m, 1361w, 1296w, 1253w, 1192w, 1163w, 1075w, 1030w, 949w, 917w, 894w, 820m, 737m, 695s, 655m, 605m. Anal. Calcd (%) for ($C_{94}H_{82}CoN_3OP_4S$) (M_w = 1484.60 g·mol^{-1}) C 76.05, H 5.57, N 2.83, S 2.16; found: C 76.34, H 5.69, N 2.82, S 1.97.

■ ASSOCIATED CONTENT

Supporting Information

The Supporting Information is available free of charge at https://pubs.acs.org/doi/10.1021/acs.inorgchem.4c00808.

NMR, UV/vis, and IR spectra for all compounds, additional experiments, proposed reaction mechanism, computational details, and crystallographic refinement (PDF)

https://doi.org/10.1021/acs.inorgchem.4c00808
Inorg. Chem. XXXX, XXX, XXX−XXX

Accession Codes

CCDC 2279472, 2279478, 2279508, 2279703, and 2325202 contain the supplementary crystallographic data for this paper. These data can be obtained free of charge via www.ccdc.cam.ac.uk/data_request/cif, or by emailing data_request@ccdc.cam.ac.uk, or by contacting The Cambridge Crystallographic Data Centre, 12 Union Road, Cambridge CB2 1EZ, UK; fax: +44 1223 336033.

AUTHOR INFORMATION

Corresponding Author

Robert Wolf − *Institute of Inorganic Chemistry, University of Regensburg, 93040 Regensburg, Germany;* orcid.org/0000-0003-4066-6483; Email: robert.wolf@ur.de

Authors

Sebastian Hauer − *Institute of Inorganic Chemistry, University of Regensburg, 93040 Regensburg, Germany;* orcid.org/0009-0009-9963-4751

Gábor Balázs − *Institute of Inorganic Chemistry, University of Regensburg, 93040 Regensburg, Germany*

Fabian Gliese − *Institute of Inorganic Chemistry, University of Regensburg, 93040 Regensburg, Germany*

Florian Meurer − *Institute of Inorganic Chemistry, University of Regensburg, 93040 Regensburg, Germany; Institute of Resource Ecology, Helmholtz-Zentrum Dresden-Rossendorf, 01314 Dresden, Germany*

Thomas M. Horsley Downie − *Institute of Inorganic Chemistry, University of Regensburg, 93040 Regensburg, Germany;* orcid.org/0000-0001-5027-450X

Christoph Hennig − *European Synchrotron Radiation Facility, Rossendorf Beamline (BM20-CRG), 38043 Grenoble, France; Institute of Resource Ecology, Helmholtz-Zentrum Dresden-Rossendorf, 01314 Dresden, Germany;* orcid.org/0000-0001-6393-2778

Jan J. Weigand − *Faculty of Chemistry and Food Chemistry, Technische Universität Dresden, 01062 Dresden, Germany;* orcid.org/0000-0001-7323-7816

Complete contact information is available at: https://pubs.acs.org/10.1021/acs.inorgchem.4c00808

Author Contributions

S. Hauer: investigation- experimental work (synthesis and characterization of the complexes), writing - original draft. G. Balázs: investigation - DFT studies, writing - review and editing. F. Gliese: investigation (synthesis and characterization of the complexes). F. Meurer and C. Hennig: investigation - collection and analysis of SCXRD data. T. M. Horsley Downie: writing - review and editing. J. J. Weigand and R. Wolf: conceptualization, supervision, writing - review and editing, funding acquisition.

Notes

The authors declare no competing financial interest.

ACKNOWLEDGMENTS

We thank Dietmar Stalke (University of Göttingen) for a generous loan of $S(NtBu)_2$ and Lisa Zimmermann (University of Regensburg) for assistance with IR measurements. Florian Meurer thanks the Studienstiftung des Deutschen Volkes for his Ph.D. fellowship. Financial support of this work by the Deutsche Forschungsgemeinschaft (DFG, grants WE4621/3-2 and WO1496/7-2) and the European Research Council (ERC CoG 772299) is gratefully acknowledged. We acknowledge the European Synchrotron Radiation Facility (ESRF) for the provision of synchrotron radiation facilities by using the ROBL beamline (BM20).

REFERENCES

(1) Reviews on the coordination chemistry of phosphorus: (a) Peruzzini, M.; Gonsalvi, L.; Romerosa, A. Coordination chemistry and functionalization of white phosphorus *via* transition metal complexes. *Chem. Soc. Rev.* **2005**, *34*, 1038−1047. (b) Caporali, M.; Gonsalvi, L.; Rossin, A.; Peruzzini, M. P_4 Activation by Late-Transition Metal Complexes. *Chem. Rev.* **2010**, *110*, 4178−4235. (c) Cossairt, B. M.; Piro, N. A.; Cummins, C. C. Early-Transition-Metal-Mediated Activation and Transformation of White Phosphorus. *Chem. Rev.* **2010**, *110*, 4164−4177. (d) Scheer, M.; Balázs, G.; Seitz, A. P_4 Activation by Main Group Elements and Compounds. *Chem. Rev.* **2010**, *110*, 4236−4256. (e) Caporali, M.; Serrano-Ruiz, M.; Peruzzini, M. Benign Chlorine-Free Approaches to Organophosphorus Compounds. In *Chemistry Beyond Chlorine*; Tundo, P., He, L.-N., Lokteva, E., Mota, C., Eds.; Springer, 2016; pp 97−136. (f) Borger, J. E.; Ehlers, A. W.; Slootweg, J. C.; Lammertsma, K. Functionalization of P_4 through Direct P−C Bond Formation. *Chem.-Eur. J.* **2017**, *23*, 11738−11746. (g) Hoidn, C. M.; Scott, D. J.; Wolf, R. Transition-Metal-Mediated Functionalization of White Phosphorus. *Chem.-Eur. J.* **2021**, *27*, 1886−1902. (h) Giusti, L.; Landaeta, V. R.; Vanni, M.; Kelly, J. A.; Wolf, R.; Caporali, M. Coordination chemistry of elemental phosphorus. *Coord. Chem. Rev.* **2021**, *441*, No. 213927.

(2) Selected examples of [1.1.0]bicyclotetraphosphane-1,4-diyl (P_4 butterfly) compounds: (a) Binger, P.; Biedenbach, B.; Krüger, C.; Regitz, M. Bis(η^5-cyclopentadienyl)-1,3-diphosphabicyclo[1.1.0]-butane-2,4-diylzirconium: A Simple Synthesis of an Unusual Molecule. *Angew. Chem., Int. Ed. Engl.* **1987**, *26*, 764−765. (b) Scherer, O. J.; Schwarz, G.; Wolmershäuser, G. Eisen-Zweikernkomplexe mit unterschiedlichen P_4-Liganden. *Z. Anorg. Allg. Chem.* **1996**, *622*, 951−957. (c) Scherer, O. J.; Hilt, T.; Wolmershäuser, G. P_4 Activation with $[\{Cp'''(OC)_2Fe\}_2]$ ($Cp''' = C_5H_2Bu^t_3$-1,2,4): Exclusive Formation of the Exo/ Exo-Butterfly Complex $[\{Cp'''(OC)_2Fe\}_2(\mu\text{-}\eta^1{:}\eta^1\text{-}P_4)]$. *Organometallics* **1998**, *17*, 4110−4112. (d) Schwarzmaier, C.; Timoshkin, A. Y.; Balázs, G.; Scheer, M. Selective Formation and Unusual Reactivity of Tetraarsabicyclo[1.1.0]butane Complexes. *Angew. Chem., Int. Ed.* **2014**, *53*, 9077−9081. (e) Pelties, S.; Herrmann, D.; de Bruin, B.; Hartl, F.; Wolf, R. Selective P_4 activation by an organometallic nickel(I) radical: formation of a dinuclear nickel(II) tetraphosphide and related di- and trichalcogenides. *Chem. Commun.* **2014**, *50*, 7014−7016. (f) Borger, J. E.; Jongkind, M. K.; Ehlers, A. W.; Lutz, M.; Slootweg, J. C.; Lammertsma, K. Metalate-Mediated Functionalization of P_4 by Trapping Anionic $[Cp^*Fe(CO)_2(\eta^1\text{-}P_4)]^-$ with Lewis Acids. *ChemistryOpen* **2017**, *6*, 350−353.

(3) Selected examples for *cyclo*-P_4 complexes: (a) Scherer, O. J.; Vondung, J.; Wolmershäuser, G. Tetraphosphacyclobutadiene as Complex Ligand. *Angew. Chem., Int. Ed. Engl.* **1989**, *28*, 1355−1357. (b) Yao, S.; Lindenmaier, N.; Xiong, Y.; Inoue, S.; Szilvási, T.; Adelhardt, M.; Sutter, J.; Meyer, K.; Driess, M. A Neutral Tetraphosphacyclobutadiene Ligand in Cobalt(I) Complexes. *Angew. Chem., Int. Ed.* **2015**, *54*, 1250−1254. (c) Dielmann, F.; Timoshkin, A.; Piesch, M.; Balázs, G.; Scheer, M. The Cobalt *cyclo*-P_4 Sandwich Complex and Its Role in the Formation of Polyphosphorus Compounds. *Angew. Chem., Int. Ed.* **2017**, *56*, 1671−1675. (d) Cavaillé, A.; Saffon-Merceron, N.; Nebra, N.; Fustier-Boutignon, M.; Mézailles, N. Synthesis and Reactivity of an End-Deck *cyclo*-P_4 Iron Complex. *Angew. Chem., Int. Ed.* **2018**, *57*, 1874−1878. (e) Mandla, K. A.; Neville, M. L.; Moore, C. E.; Rheingold, A. L.; Figueroa, J. S. Dianionic Mononuclear *Cyclo*-P_4 Complexes of Zero-Valent Molybdenum: Coordination of the *Cyclo*-P_4 Dianion in the Absence of Intramolecular Charge Transfer. *Angew. Chem., Int. Ed.* **2019**, *58*, 15329−15333. (f) Mandla, K. A.; Moore, C. E.; Rheingold, A. L.; Figueroa, J. S. Photolytic Reductive Elimination of White Phosphorus from a Mononuclear *cyclo*-P_4 Transition Metal Complex. *Angew. Chem., Int. Ed.* **2019**, *58*, 1779−1783. (g) Hoidn, C. M.; Maier, T. M.; Trabitsch,

https://doi.org/10.1021/acs.inorgchem.4c00808
Inorg. Chem. XXXX, XXX, XXX−XXX

K.; Weigand, J. J.; Wolf, R. [3 + 2] Fragmentation of a Pentaphosphido Ligand by Cyanide. *Angew. Chem., Int. Ed.* **2019**, *58*, 18931−18936.
(4) (a) Scherer, O. J.; Hilt, T.; Wolmershäuser, G. [$Cp^R(OC)_2Fe_2(\mu$-η^1:η^1-P_4)]: Starting Material for the Synthesis of Iron Sandwich Compounds with a 1,2,3-Triphospholyl Ligand and of a Trinuclear Iron Complex with a P_{11} Ligand. *Angew. Chem., Int. Ed.* **2000**, *39*, 1425−1427. (b) Scheer, M.; Deng, S.; Scherer, O. J.; Sierka, M. Tetraphosphacyclopentadienyl and Triphosphaallyl Ligands in Iron Complexes. *Angew. Chem., Int. Ed.* **2005**, *44*, 3755−3758. (c) Schwarzmaier, C.; Bodensteiner, M.; Timoshkin, A. Y.; Scheer, M. An Approach to Mixed P_nAs_m Ligand Complexes. *Angew. Chem., Int. Ed.* **2014**, *53*, 290−293. (d) Schwarzmaier, C.; Heinl, S.; Balázs, G.; Scheer, M. E_4 Butterfly Complexes (E = P, As) as Chelating Ligands. *Angew. Chem., Int. Ed.* **2015**, *54*, 13116−13121. (e) Seitz, A. E.; Eckhardt, M.; Erlebach, A.; Peresypkina, E. V.; Sierka, M.; Scheer, M. Pnictogen−Silicon Analogues of Benzene. *J. Am. Chem. Soc.* **2016**, *138*, 10433−10436. (f) Borger, J. E.; Ehlers, A. W.; Lutz, M.; Slootweg, J. C.; Lammertsma, K. Selective [3 + 1] Fragmentations of P_4 by "P" Transfer from a Lewis Acid Stabilized $[RP_4]^-$ Butterfly Anion. *Angew. Chem., Int. Ed.* **2017**, *56*, 285−290. (g) Müller, J.; Heinl, S.; Schwarzmaier, C.; Balázs, G.; Keilwerth, M.; Meyer, K.; Scheer, M. Rearrangement of a P_4 Butterfly Complex—The Formation of a Homoleptic Phosphorus−Iron Sandwich Complex. *Angew. Chem., Int. Ed.* **2017**, *56*, 7312−7317. (h) Borger, J. E.; Jongkind, M. K.; Ehlers, A. W.; Lutz, M.; Slootweg, J. C.; Lammertsma, K. Metalate-Mediated Functionalization of P_4 by Trapping Anionic $[Cp^*Fe(CO)_2(\eta^1$-$P_4)]^-$ with Lewis Acids. *ChemistryOpen* **2017**, *6*, 350−353. (i) Grünbauer, R.; Balázs, G.; Scheer, M. The Butterfly Complex $[\{Cp^*Cr(CO)_3\}_2(\mu,\eta^{1:1}$-$P_4)]$ as a Versatile Ligand and Its Unexpected P_1/P_3 Fragmentation. *Chem.-Eur. J.* **2020**, *26*, 11722−11726. (j) Reichl, S.; Grünbauer, R.; Balázs, G.; Scheer, M. Reactivity of P_4 Butterfly Complexes towards NHCs − generation of a metal-bridged P_2 dumbbell complex. *Chem. Commun.* **2021**, *57*, 3383−3386. (k) Grünbauer, R.; Schwarzmaier, C.; Eberl, M.; Balázs, G.; Scheer, M. The reactivity of the P_4-butterfly ligand $[\{Cp'''Fe(CO)_2\}_2(\mu,\eta^{1:1}$-$P_4)]$ towards transition metal complexes: Coordination versus rearrangement. *Inorg. Chim. Acta* **2021**, *518*, No. 120234. (l) Weber, M.; Balázs, G.; Virovets, A. V.; Peresypkina, E.; Scheer, M. Insertion of Phosphenium Ions into a Bicyclo[1.1.0]-Tetraphosphabutane Iron Complex. *Molecules* **2021**, *26*, 3920.
(5) Pelties, S.; Ehlers, A. W.; Wolf, R. Insertion of phenyl isothiocyanate into a P−P bond of a nickel-substituted bicyclo[1.1.0]-tetraphosphabutane. *Chem. Commun.* **2016**, *52*, 6601−6604.
(6) Piesch, M.; Seidl, M.; Scheer, M. Transformations of the *cyclo*-P_4 ligand in $[Cp'''Co(\eta^4$-$P_4)]$. *Chem. Sci.* **2020**, *11*, 6745−6751.
(7) Hauer, S.; Horsley Downie, T. M.; Balázs, G.; Schwedtmann, K.; Weigand, J. J.; Wolf, R. Cobalt-Mediated [3 + 1] Fragmentation of White Phosphorus: Access to Acylcyanophosphanides. *Angew. Chem., Int. Ed.* **2024**, *63*, No. e202317170.
(8) (a) Chakraborty, U.; Leitl, J.; Mühldorf, B.; Bodensteiner, M.; Pelties, S.; Wolf, R. Mono- and dinuclear tetraphosphabutadiene ferrate anions. *Dalton Trans.* **2018**, *47*, 3693−3697. (b) Hoidn, C. M.; Rödl, C.; McCrea-Hendrick, M. L.; Block, T.; Pöttgen, R.; Ehlers, A. W.; Power, P. P.; Wolf, R. Synthesis of a Cyclic Co_2Sn_2 Cluster Using a Co^- Synthon. *J. Am. Chem. Soc.* **2018**, *140*, 13195−13199. (c) Ziegler, C. G. P.; Maier, T. M.; Pelties, S.; Taube, C.; Hennersdorf, F.; Ehlers, A. W.; Weigand, J. J.; Wolf, R. Construction of alkyl-substituted pentaphosphido ligands in the coordination sphere of cobalt. *Chem. Sci.* **2019**, *10*, 1302−1308. (d) Adhikari, A. K.; Ziegler, C. G. P.; Schwedtmann, K.; Taube, C.; Weigand, J. J.; Wolf, R. Functionalization of Pentaphosphorus Cations by Complexation. *Angew. Chem., Int. Ed.* **2019**, *58*, 18584−18590.
(9) Calculated single- and double-bond lengths: (a) Pyykkö, P.; Atsumi, M. Molecular Single-Bond Covalent Radii for Elements 1−118. *Chem.-Eur. J.* **2009**, *15*, 186−197. (b) Pyykkö, P.; Atsumi, M. Molecular Double-Bond Covalent Radii for Elements Li−E112. *Chem.-Eur. J.* **2009**, *15*, 12770−12779.
(10) Bianchini, C.; Masi, D.; Mealli, C. C.; Meli, A. Structural Comparison of Cobalt and Nickel Complexes with CS_2 and SCNPh molecules Stabilized by Tripodal Polyphosphine Ligands. Implications for the Nature of the Chemical Bonding in Compounds Containing C−S linkages η^2 Coordinated to L_3M Fragments. *Inorg. Chem.* **1984**, *23*, 2838−2844.
(11) Piesch, M.; Reichl, S.; Seidl, M.; Balázs, G.; Scheer, M. Synthesis and Multiple Subsequent Reactivity of Anionic *cyclo*-E_3 Ligand Complexes (E = P, As). *Angew. Chem., Int. Ed.* **2021**, *60*, 15101−15108.
(12) Scheinost, A. C.; Claussner, J.; Exner, J.; Feig, M.; Findeisen, S.; Hennig, C.; Kvashnina, K. O.; Naudet, D.; Prieur, D.; Rossberg, A.; Schmidt, M.; Qiu, C.; Colomp, P.; Cohen, C.; Dettona, E.; Dyadkin, V.; Stumpf, T. ROBL-II at ESRF: a synchrotron toolbox for actinide research. *J. Synchrotron Radiat.* **2021**, *28*, 333−349.
(13) Related cyclic P_4N frameworks: (a) Issleib, K.; Rockstroh, Ch.; Duchek, I.; Fluck, E. Alkali-Phosphorverbindungen und ihr reaktives Verhalten. LV. Alkalimetall- bzw. Magnesium-tetra- und -pentaalkylphosphine. *Z. Anorg. Allg. Chem.* **1968**, *360*, 77−87. (b) Baudler, M.; Vesper, J.; Junkes, P.; Sandmann, H. A Novel Phosphorus Heterocycle: 1,2,3,4-Tetraphenyl-1,2,3,4-tetraphospholane. *Angew. Chem., Int. Ed. Engl.* **1971**, *10*, 940−940. (c) Baudler, M.; Tolls, E.; Clef, E.; Kloth, B.; Koch, D. Beiträge zur Chemie des Phosphors. 72. Über die Alkylcyclomonocarbaphosphane $(PR)_4CH_2$, R = CH_3, C_2H_5, t-C_4H_9. *Z. Anorg. Allg. Chem.* **1977**, *435*, 21−32. (d) Baudler, M.; Lütkecosmann, P. Beiträge zur Chemie des Phosphors. 99. Ein Heterocyclophosphan mit P_4N-Ringgerüst: Synthese und Eigenschaften von $(PC_6H_5)_4N$(c-C_6H_{11}). *Z. Anorg. Allg. Chem.* **1981**, *472*, 38−44. (e) Hinz, A.; Schulz, A.; Villinger, A. New P−N Cage Compounds Generated by Small-Molecule Activation. *Chem.-Eur. J.* **2014**, *20*, 3913−3916. (f) Kosnik, S. C.; Farrar, G. J.; Norton, E. L.; Cooper, B. F. T.; Ellis, B. D.; Macdonald, C. L. B. Low-Valent Chemistry: An Alternative Approach to Phosphorus-Containing Oligomers. *Inorg. Chem.* **2014**, *53*, 13061−13069. (g) Dielmann, F.; Bertrand, G. Reactivity of a Stable Phosphinonitrene towards Small Molecules. *Chem.-Eur. J.* **2015**, *21*, 191−198. (h) Höhne, M.; Joksch, M.; Konieczny, K.; Müller, B. H.; Spannenberg, A.; Peulecke, N.; Rosenthal, U. Selective Reductions of *N*,*N*-Bischloro(aryl)-phosphino-amines Yielding Three-, Five-, Six-, and Eight-Membered Cyclic Azaphosphanes. *Chem.-Eur. J.* **2017**, *23*, 4298−4309. (i) Bresien, J.; Hinz, A.; Schulz, A.; Villinger, A. As−N and As−N−P Cage Compounds Generated by [2 + 2] Addition of Diazenes and Diphosphenes to Diarsadiazanediyls. *Eur. J. Inorg. Chem.* **2018**, *2018*, 1679−1682.
(14) (a) Weigend, F.; Häser, M.; Patzelt, H.; Ahlrichs, R. RI-MP2: optimized auxiliary basis sets and demonstration of efficiency. *Chem. Phys. Lett.* **1998**, *294*, 143−152. (b) Tao, J.; Perdew, J. P.; Staroverov, V. N.; Scuseria, G. E. Climbing the Density Functional Ladder: Nonempirical Meta−Generalized Gradient Approximation Designed for Molecules and Solids. *Phys. Rev. Lett.* **2003**, *91*, No. 146401. (c) Staroverov, V. N.; Scuseria, G. E.; Tao, J.; Perdew, J. P. Comparative assessment of a new nonempirical density functional: Molecules and hydrogen-bonded complexes. *J. Chem. Phys.* **2003**, *119*, 12129−12137. (d) Staroverov, V. N.; Scuseria, G. E.; Tao, J.; Perdew, J. P. Erratum: "Comparative assessment of a new nonempirical density functional: molecules and hydrogen-bonded complexes" [J. Chem. Phys. 119, 12129 (2003)]. *J. Chem. Phys.* **2004**, *121*, 11507. (e) Weigend, F.; Ahlrichs, R. Balanced basis sets of split valence, triple zeta valence and quadruple zeta valence quality for H to Rn: Design and assessment of accuracy. *Phys. Chem. Chem. Phys.* **2005**, *7*, 3297−3305. (f) Tomasi, J.; Mennucci, B.; Cammi, R. Quantum Mechanical Continuum Solvation Models. *Chem. Rev.* **2005**, *105*, 2999−3094. (g) Weigend, F. Accurate Coulomb-fitting basis sets for H to Rn. *Phys. Chem. Chem. Phys.* **2006**, *8*, 1057−1065. (h) Caldeweyher, E.; Bannwarth, C.; Grimme, S. Extension of the D3 dispersion coefficient model. *J. Chem. Phys.* **2017**, *147*, No. 034112. (i) Caldeweyher, E.; Ehlert, S.; Hansen, A.; Neugebauer, H.; Spicher, S.; Bannwarth, C.; Grimme, S. A generally applicable atomic-charge dependent London dispersion correction. *J. Chem. Phys.* **2019**, *150*, No. 154122.
(15) Related *catena*-P_4 units: (a) Scherer, O. J.; Berg, G.; Wolmershäuser, G. Ligandgesteuerte P_2-verknüpfung zu einem acyclischen P_4-liganden. *Chem. Ber.* **1995**, *128*, 635−639. (b) Barbaro, P.; Di Vaira, M.; Peruzzini, M.; Seniori Costantini, S.; Stoppioni, P. Getting a Clue to the Hydrolytic Activation of White Phosphorus: The

https://doi.org/10.1021/acs.inorgchem.4c00808
Inorg. Chem. XXXX, XXX, XXX−XXX

Generation and Stabilization of $P(OH)_2PHPHPH(OH)$ at Ruthenium Centers. *Inorg. Chem.* **2009**, *48*, 1091−1096. (c) Piesch, M.; Seidl, M.; Stubenhofer, M.; Scheer, M. Ring Expansions of Nonpolar Polyphosphorus Rings. *Chem.-Eur. J.* **2019**, *25*, 6311−6316. (d) Müller, J.; Balázs, G.; Scheer, M. From a P_4 butterfly scaffold to *cyclo*- and *catena*-P_4 units. *Chem. Commun.* **2021**, *57*, 2257−2260.

(16) Herberhold, M.; Gerstmann, S.; Wrackmeyer, B.; Borrmann, H. Solid-state structure of sulfur bis(trimethylsilylimide), $S(NSiMe_3)_2$, and multinuclear magnetic resonance studies of some sulfur bis(silylimides) in solution. *J. Chem. Soc., Dalton Trans.* **1994**, 633−636.

(17) (a) Weber, L.; Uthmann, S.; Bögge, H.; Müller, A.; Stammler, H.-G.; Neumann, B. Synthesis, Structure, and Coordination Chemistry of P-Acyl-, P-Thiocarbamoyl-, and P-Dithiocarboxyl-Substituted Phosphaalkenes $R(X)C{-}PC(NMe_2)_2$ (R = Ph, *t*Bu, $SSiMe_3$, $N(Ph)SiMe_3$; X = O, S). *Organometallics* **1998**, *17*, 3593−3598. (b) Barluenga, J.; Rubio, E.; Tomás, M. 6.18 - Functions Containing a Thiocarbonyl Group Bearing Two Heteroatoms Other Than a Halogen or Chalcogen. In *Comprehensive Organic Functional Group Transformations II*; Katritzky, A. R., Taylor, R. J. K., Eds.; Elsevier: Oxford, 2005; pp 545−572.

(18) Socrates, G. *Infrared and Raman Characteristic Group Frequencies: Tables and Charts*; Wiley: Chichester, 2004.

(19) Laliberté, D.; Maris, T.; Wuest, J. D. Molecular tectonics − Use of urethanes and ureas derived from tetraphenylmethane and tetraphenylsilane to build porous chiral hydrogen-bonded networks. *Can. J. Chem.* **2004**, *82*, 386−398.

(20) Khusniyarov, M. M.; Harms, K.; Burghaus, O.; Sundermeyer, J. Molecular and Electronic Structures of Homoleptic Nickel and Cobalt Complexes with Non-Innocent Bulky Diimine Ligands Derived from Fluorinated 1,4-Diaza-1,3-Butadiene (DAD) and Bis(arylimino)-acenaphthene (BIAN). *Eur. J. Inorg. Chem.* **2006**, *2006*, 2985−2996.

(21) Budzelaar, P. H. M. gNMR for Windows (5.0.6.0) NMR Simulation Program, IvorySoft, 2006.

(22) (a) Finer, E. G.; Harris, R. K. N.M.R. Spectra of the $X_nAA'X_n'$ Type. *Mol. Phys.* **1967**, *13*, 65−75. (b) Aime, S.; Harris, R. K.; McVicker, E. M.; Fild, M. Multinuclear magnetic resonance studies. Part 2. Diphosphanes and dithioxodi- λ^5-phosphanes. *J. Chem. Soc., Dalton Trans.* **1976**, 2144−2153. (c) Albrand, J. P.; Faucher, H.; Gagnaire, D.; Robert, J. B. Calculation of the ^1J(PP) Angular Dependence in P_2H_4. *Chem. Phys. Lett.* **1976**, *38*, 521−523. (d) McFarlane, H. C. E.; McFarlane, W.; Nash, J. A. Phosphorus−Phosphorus Nuclear Spin Coupling in Tetraorganobiphosphines and Some of Their Derivatives. *J. Chem. Soc., Dalton Trans.* **1980**, 240−244. (e) Forgeron, M. A. M.; Gee, M.; Wasylishen, R. E. A Theoretical Investigation of One-Bond Phosphorus−Phosphorus Indirect Nuclear Spin−Spin Coupling Tensors, $^1J(^{31}P,^{31}P)$, Using Density Functional Theory. *J. Phys. Chem. A* **2004**, *108*, 4895−4908. (f) Del Bene, J. E.; Elguero, J.; Alkorta, I. Computed Spin−Spin Coupling Constants ($^1J_{X\text{-}Y}$) in Molecules $H_mX{-}YH_n$ for X and Y = ^{13}C, ^{15}N, and ^{31}P: Comparisons with Experiment and Insights into the Signs of $^1J_{X\text{-}Y}$. *J. Phys. Chem. A* **2004**, *108*, 3662−3667.

https://doi.org/10.1021/acs.inorgchem.4c00808
Inorg. Chem. XXXX, XXX, XXX−XXX